

Electronic Supplementary Information (ESI)

Remarkably Enhanced Ion-Exchange Capacity of H₂O₂- Intercalated Layered Titanate

Experimental

The starting material of the layered titanate H_{1.07}Ti_{1.73}O₄·H₂O (HTO) with platelike morphology was prepared using the method described in the literature¹. 0.5g of HTO were put in 100 mL of 30 wt% H₂O₂ solution and stirred for 10 min at room temperature, and then were filtered, washed with distilled water to obtain the H₂O₂-treated HTO (named as H₂O₂-HTO). H₂O₂-HTO was treated in a 0.3 100mL M(CH₃COO)₂ (M=Co, Ni, Cu and Zn) solution for different stirring times at room temperature. After the treatment, the M²⁺-ion-exchanged samples were filtered, washed with large amount of distilled water to remove the excess of ions on the surface of samples by physic adsorption, and dried at room temperature (named as M-H₂O₂-HTO). In comparison, HTO was also treated in the M(CH₃COO)₂ (M=Co, Ni, Cu and Zn) solution under the same conditions and obtained sample is named as M-HTO.

Rapid ion exchange experiments

0.5g of H₂O₂-HTO was treated in 0.3 mol/L 100mL M(CH₃COO)₂ (M=Co, Ni, Cu, Zn) solution respectively under constant stirring at ambient temperature for 40 min, and the solution was replaced after 10 min of reaction to ensure complete ion exchange. The samples were filtered, washed with large amount of distilled water to remove the excess of ions by physic adsorption and dried in air to obtain M ion-exchanged H₂O₂-HTO products.

Characterization

The crystal structure of the sample was investigated using a powder X-ray diffractometer (XRD, Rigaku D/max-2200PC) with Cu Ka ($\lambda=0.15418$ nm) radiation. The size and morphology of the samples were observed using a field-emission scanning electron microscope (Hitachi, FE-SEM, S-4800). Transmission electron microscopy (TEM) and selected-area electron diffraction (SAED) were performed on a Tecnai G2F20STWIN system at 200 kV, and the powder sample was supported on a microgrid. X-ray fluorescence (XRF, Horiba XGT-7200) was conducted to analyze the elements

distribution of samples. X-ray photoelectron spectroscopy (XPS) measurements were carried out by an Axis Ultra XPS instrument with an Al Ka X-ray source, and the spectra were calibrated to the C 1s peak at 284.6 eV. The Fourier transform infrared (FT-IR) spectra were measured in Bruker infrared spectrometer (VERTE70) with the KBr disk technique. Electron spin resonance (ESR, Bruker A300-9.5/12) spectra were tested to observe the single-electron in the samples.

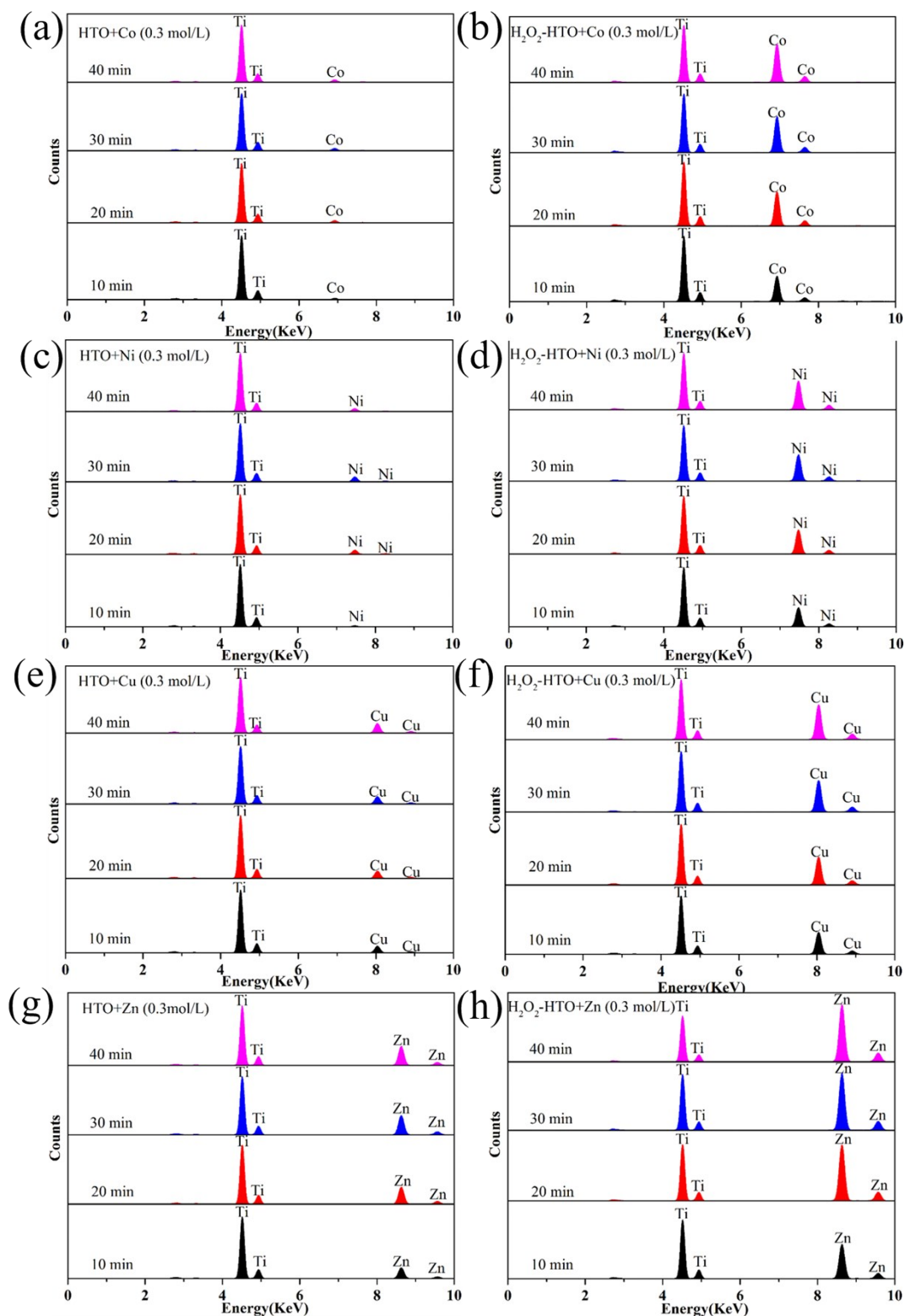


Fig. S1 XRF spectra of products obtained by ion-exchange treatments of (a, c, e, g) HTO and (b, d, f, h)

H_2O_2 -HTO with Co^{2+} , Ni^{2+} , Cu^{2+} and Zn^{2+} (0.3mol/L) within 40 min.

Table S1 The change of pH and M²⁺ content (M/Ti) before and after ion exchange treatment within 40 min.

Ions	Exchange time	HTO			H ₂ O ₂ -HTO		
		pH		M/Ti(At%)	pH		M/Ti(At%)
		Before	After		Before	After	
Co ²⁺	10min	7.87	7.34	0.033:1.73	7.87	6.38	0.55:1.73
	20min	7.87	7.51	0.053:1.73	7.87	6.85	0.74:1.73
	30min	7.87	7.57	0.064:1.73	7.87	7.15	0.83:1.73
	40min	7.87	7.65	0.068:1.73	7.87	7.44	0.91:1.73
Ni ²⁺	10min	7.73	7.51	0.022:1.73	7.73	6.77	0.39:1.73
	20min	7.73	7.59	0.088:1.73	7.73	7.47	0.49:1.73
	30min	7.73	7.62	0.104:1.73	7.73	7.47	0.56:1.73
	40min	7.73	7.56	0.064:1.73	7.73	7.58	0.59:1.73
Cu ²⁺	10min	5.80	5.78	0.105:1.73	5.80	5.72	0.36:1.73
	20min	5.80	5.80	0.114:1.73	5.80	5.81	0.42:1.73
	30min	5.80	5.83	0.122:1.73	5.80	5.00	0.48:1.73
	40min	5.80	5.76	0.168:1.73	5.80	5.83	0.53:1.73
Zn ²⁺	10min	6.97	6.86	0.145:1.73	6.97	6.48	0.46:1.73
	20min	6.97	6.95	0.235:1.73	6.97	5.79	0.75:1.73
	30min	6.97	6.96	0.268:1.73	6.97	6.89	0.78:1.73
	40min	6.97	7.01	0.257:1.73	6.97	6.99	0.93:1.73

Table S2 The change of pH and M²⁺ content (M/Ti) before and after ion exchange treatment for 48h.

Ions	HTO			H ₂ O ₂ -HTO		
	pH		M/Ti(At%)	pH		M/Ti(At%)
	Before	After		Before	After	
Co ²⁺	7.87	7.50	0.18:1.73	7.87	5.67	1.07:1.73

Ni ²⁺	7.73	7.66	0.08:1.73	7.73	6.77	0.61:1.73
Cu ²⁺	5.80	5.98	0.24:1.73	5.80	6.13	0.64:1.73
Zn ²⁺	6.97	6.75	0.51:1.73	6.97	5.92	1.07:1.73
Mn ²⁺	6.80	5.88	0.31:1.73	6.80	5.28	0.97:1.73
Ca ²⁺	6.35	5.74	0.17:1.73	6.35	5.43	0.21:1.73
Mg ²⁺	8.49	6.58	0.26:1.73	8.49	6.40	0.48:1.73
Ba ²⁺	7.50	5.98	0.03:1.73	7.50	6.13	0.04:1.73
Sr ²⁺	8.06	6.55	0.124:1.73	8.06	6.93	0.305:1.73
Cd ²⁺	6.23	5.54	0.25:1.73	6.23	5.45	0.12:1.73
Cr ³⁺	3.90	3.38	0.01:1.73	3.90	3.68	0.04:1.73

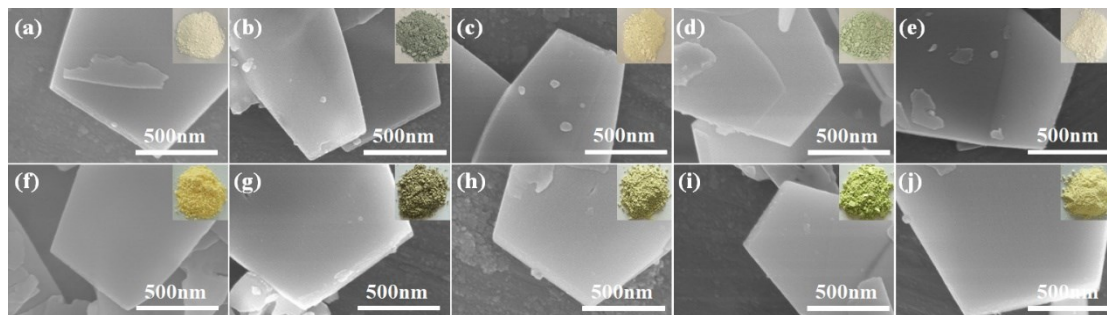


Fig. S2 SEM images and optical photos of (a) HTO, (b) Co-HTO, (c) Ni-HTO, (d) Cu-HTO, (e) Zn-HTO, (f) H₂O₂-HTO, (g) Co-H₂O₂-HTO, (h) Ni-H₂O₂-HTO, (i) Cu-H₂O₂-HTO and (j) Zn-H₂O₂-HTO.

Table S3 Zeta potential of HTO before and after the H₂O₂ treatment.

Sample	Zeta potential (mV)
HTO	-581 mV (ethanol system)
	-26.3 mV (water system)
H ₂ O ₂ -HTO	-3.31X10 ⁴ mV (ethanol system)
	-41.9 (water system)

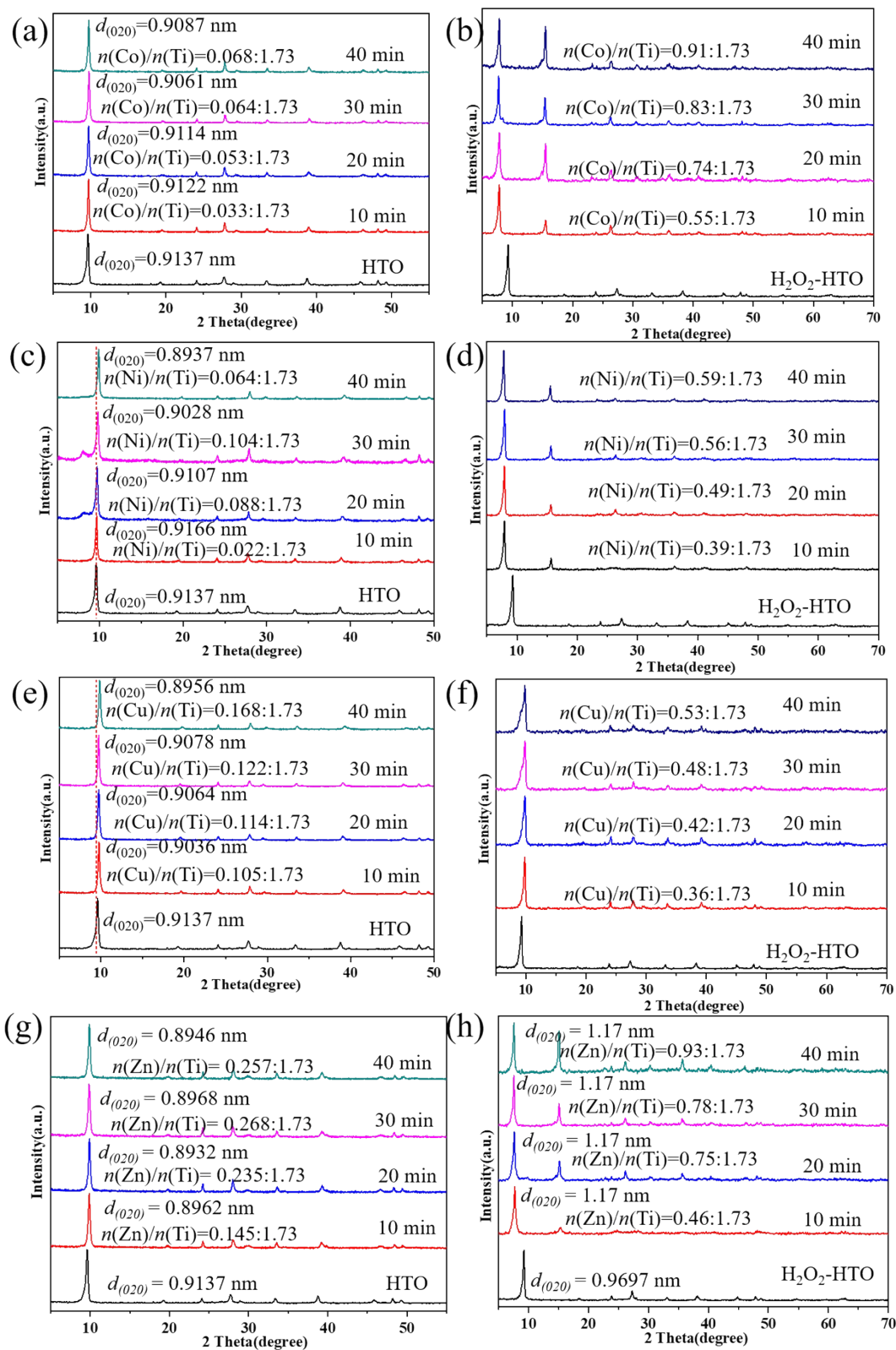


Fig. S3 XRD patterns of products obtained by ion-exchange treatments of (a, c, e, g) HTO and (b, d, f, h)

$\text{H}_2\text{O}_2\text{-HTO}$ with Co^{2+} , Ni^{2+} , Cu^{2+} and Zn^{2+} within 40 min.

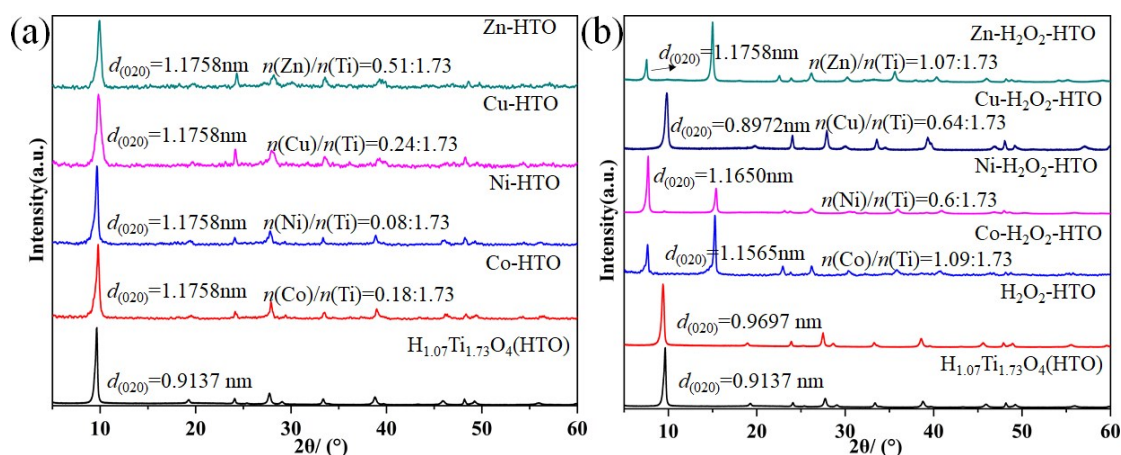


Fig. S4 XRD patterns of products obtained by ion-exchange treatments of (a) HTO and (b) H_2O_2 -HTO with Co^{2+} , Ni^{2+} , Cu^{2+} and Zn^{2+} for 48h.

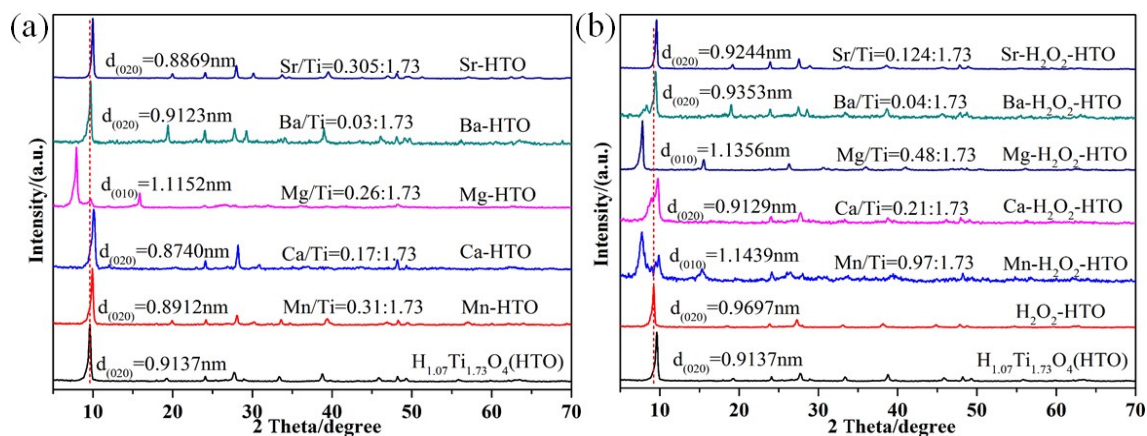


Fig. S5 XRD patterns of products obtained by ion-exchange treatments of HTO (a) and H_2O_2 -HTO (b) with Mn^{2+} , Ca^{2+} , Mg^{2+} , Ba^{2+} and Sr^{2+} for 48h

Table S4 Refined structural parameters of HTO and H_2O_2 -HTO before and after ion-exchanged-treatments.

Sample	Crystal system	a (Å)	b (Å)	c (Å)	Space group	Rp (%)	Rwp (%)
HTO	orthorhombic	3.78335	18.3246	3.00172	Ima2	8.76	8.72
H_2O_2 -HTO	orthorhombic	3.79939	18.6295	2.98932	Ima2	6.00	5.97
Zn-HTO	orthorhombic	3.75781	17.9772	7.11390	Ima2	8.29	8.32
Zn- H_2O_2 -HTO	orthorhombic	3.77615	23.7187	2.97914	Ima2	5.45	6.08

Co-H ₂ O ₂ -HTO	orthorhombic	3.78593	23.2067	2.98551	Ima2	9.58	9.80
Ni-H ₂ O ₂ -HTO	orthorhombic	3.80627	23.1777	2.98154	Ima2	7.62	7.53
Cu-H ₂ O ₂ -HTO	orthorhombic	3.78562	17.8442	2.98609	Ima2	9.77	6.54

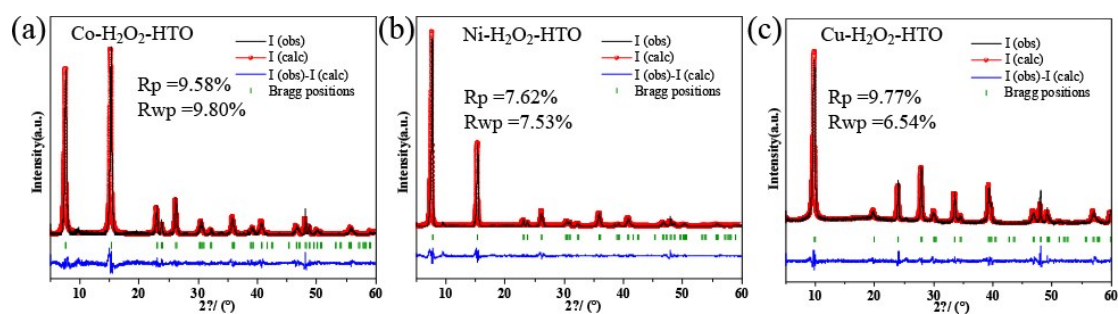


Fig. S6 Experimental XRD patterns (solid lines) and refinement fitting patterns (red line) of (a) Co-H₂O₂-HTO, Ni-(b) H₂O₂-HTO and (c) Cu-H₂O₂-HTO.

Measurement of H₂O₂ content in H₂O₂-HTO by XPS

XPS was employed to further confirm the existence of O-O bond before and after ion exchange, as shown in Fig. S7, where the binding energies were calibrated for specimens charging by referencing the C 1s to 284.60 eV. It is found that no peaks of other elements except C, O, Zn along with Ti were observed in the survey spectra (Fig. S7(A-a)). HTO shows two peaks in the O1s spectrum (Fig. S7(B-a)). The peak at 529.91 eV is assigned to the O1s of Ti-O bond in TiO₆ octahedral layer and the peak located at 530.93 eV to the O1s of interlayer H₂O. After H₂O₂ treatment, the XPS spectrum shows three peaks in the O1s spectrum (Fig. S7(B-b)). Except peaks of Ti-O bond and interlayer H₂O, a O1s peak of -O-O- bond located at 531.90 eV was observed in H₂O₂-HTO.² The results suggest H₂O₂ was intercalated into HTO after H₂O₂ treatment.

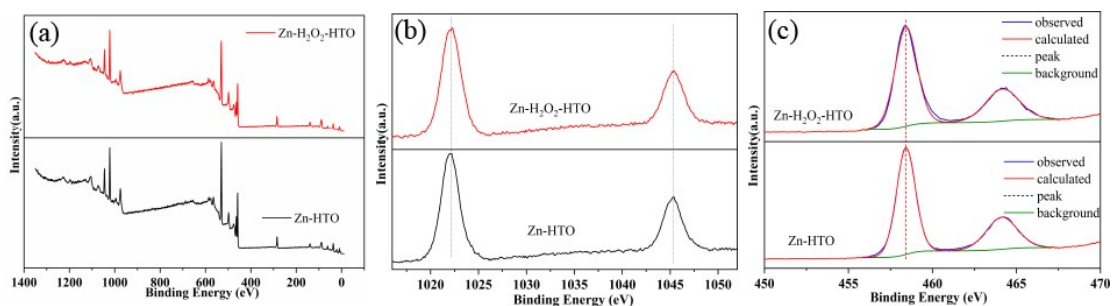


Fig. S7(A) (a) XPS survey spectra, (b) Zn2p, and (c) Ti2p XPS spectra of Zn-HTO and Zn-H₂O₂-HTO

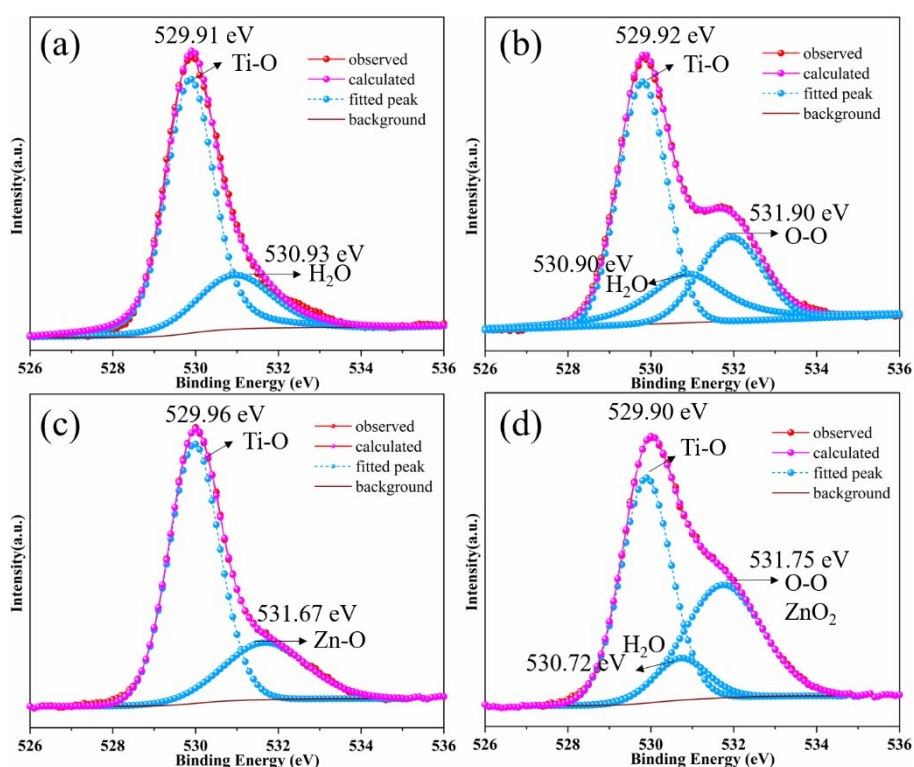


Fig. S7(B) The resolution binding energy spectra of O1s of (a) HTO, (b) H₂O₂-HTO, (c) Zn-HTO and (d) Zn-H₂O₂-HTO.

The O1s spectrum of Zn-HTO can be fitted to two peaks located at 529.96 and 531.67 eV (Fig. 7(B-c)), which correspond to the Ti-O bond in TiO₆ octahedral layer, and Zn-O formed by ion-exchange, respectively. No peak of H₂O is found in Zn-HTO, indicating that the loss of H₂O during H⁺/Zn²⁺ ion exchange in HTO. The O1s spectrum of Zn-H₂O₂-HTO can be fitted to three peaks (Fig. 7(B-d)), and the peak at 529.90 eV is attributed to Ti-O bond in TiO₆ octahedral layer while the peak at 531.75 eV corresponds to O-O bond in the interlayer of Zn-H₂O₂-HTO. Besides, a clear peak is observed at 530.72 eV, attributing to the existence of interlayer H₂O. It shows that H₂O molecules

within interlayer still exist before and after H₂O₂-HTO ion exchanging with Zn²⁺, which differs with Zn-HTO. Zn2p spectra of Zn-HTO and Zn-H₂O₂-HTO are almost the same, and the binding energy appeared at 1022.00 eV indicates the presence of Zn(II) (Fig. S7(A-b)).³ The peaks located at 458.41 eV and 464.19 eV are assigned to Ti2p 2/3 and Ti2p 1/2, respectively, showing the existence of Ti(IV) (Fig. S7(A-c)). The XPS analysis further confirmed the existence of O-O bond before and after ion exchange treatment, and also suggest that the valence of exchanged cation and Ti in TiO₆ octahedron layer has no change before and after ion exchange.

Based on the XPS analyses, various atom contents (atom %) in H₂O₂-HTO can be evaluated from the peak areas of the XPS spectrum, as shown in Table S5. The chemical formula of H₂O₂-HTO can be expressed as H_{1.07}Ti_{1.73}O_{3.6}(-O-O-H)_{0.8}•1.5H₂O, in which ion-exchangeable H⁺ content can be estimated to be about H/Ti=1.87:1.73 by assuming that all H⁺ ions in H_{1.07}Ti_{1.73}O_{3.6}(-O-O-H)_{0.8} are ion-exchangeable. Therefore, the theoretical ion-exchange capacity for M²⁺ is about M/Ti=0.94:1.73 that is close to Zn content in Zn-H₂O₂-HTO. Therefore, the theoretical ion-exchange capacity of H₂O₂-HTO for divalent ions (M/Ti= 0.94:1.73) is much larger than that of HTO (M/Ti=0.54:1.73).

Table S5 The contents of C1s, Ti2p and O1s calculated from XPS spectra of H₂O₂-HTO

Name	Peak BE	FWHM eV	Area (P)	Atomic %
C1s	284.49	1.94	20545.61	19.31
Ti2p	458.47	1.36	99987.27	15.37
O1s of Ti-O	529.92	1.36	102311.1	36.31
O1s of H ₂ O	531.90	1.64	44099.63	15.66
O1s of -O-O-	530.90	1.16	13042.29	13.34

Table S6 The molar ratios of Zn/Ti in different layered tianates obtained by ion-exchanging treatments with Zn^{2+} for 48 h and theoretical exchange capacities

Sample	Measured exchange capacity (Zn/Ti) for Zn^{2+}	Theoretical exchange capacity (Zn/Ti) for Zn^{2+}
H_2O_2 -treated $\text{H}_{1.07}\text{Ti}_{1.73}\text{O}_4$ (H_2O_2 -HTO)	0.62	0.62
$\text{H}_{1.07}\text{Ti}_{1.73}\text{O}_4$ (HTO)	0.29	0.31
$\text{H}_2\text{Ti}_2\text{O}_5$	0.27	0.5
$\text{H}_2\text{Ti}_3\text{O}_7$	0.0067	0.33
$\text{H}_2\text{Ti}_4\text{O}_9$	0.16	0.25
$\text{H}_2\text{Ti}_5\text{O}_{11}$	0.19	0.2

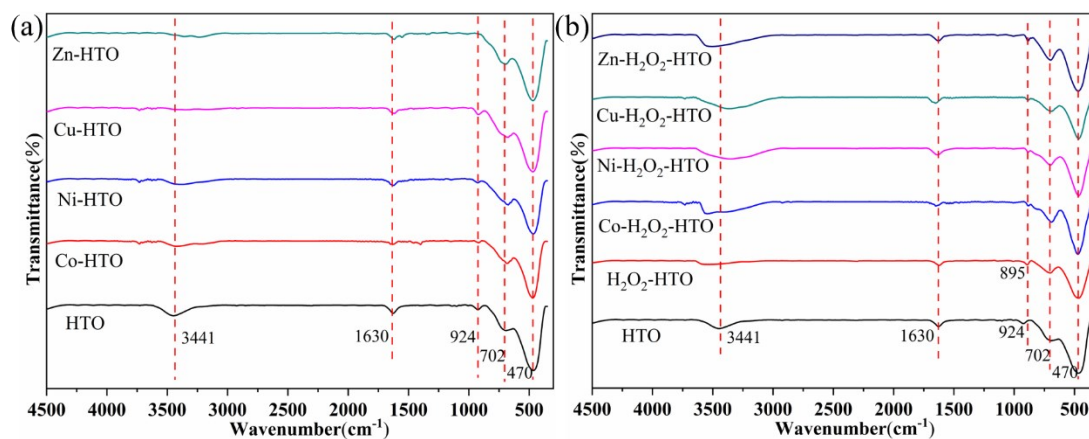


Fig. S8 FT-IR spectra of HTO, H_2O_2 -HTO, M-HTO and M- H_2O_2 -HTO.

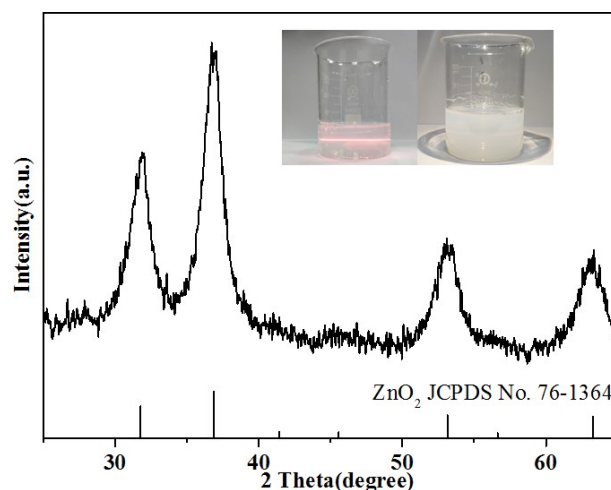


Fig. S9 XRD pattern of product obtained by reaction of H₂O₂ reacting and Zn(CH₃COO)₂ solutions and optical photos of solution change before and reaction.

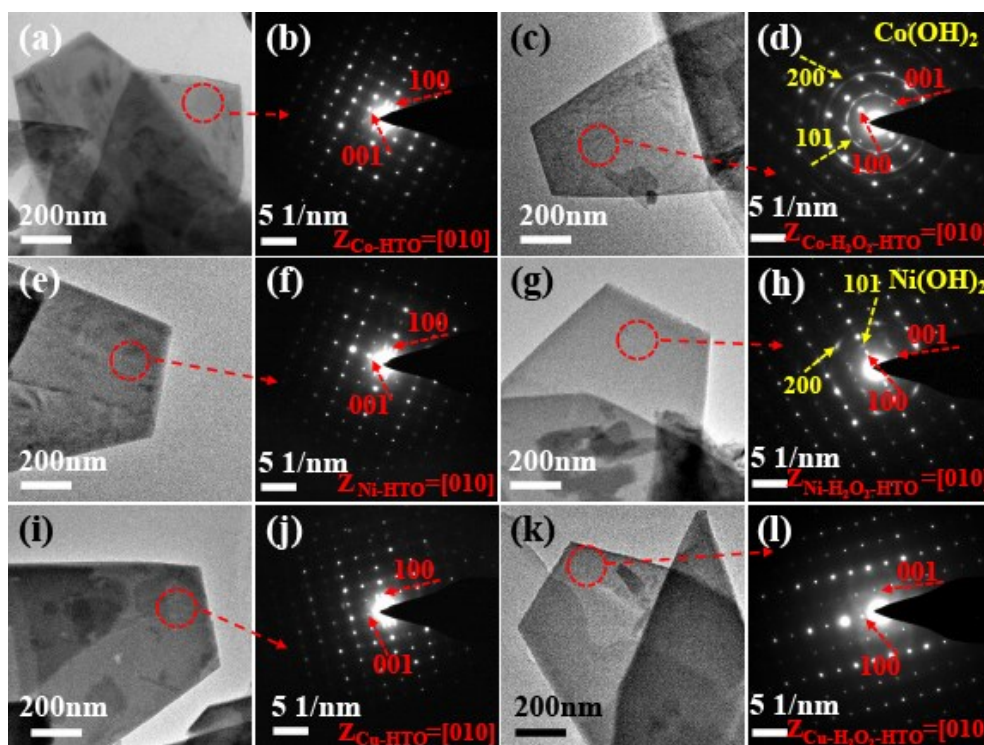


Fig. S10 TEM images and SAED patterns of (a)(b) Co-HTO(c)(d) Ni-HTO (e)(f) Cu-HTO (g)(h) Zn-HTO

TEM images show that Co-HTO, Ni-HTO and Cu-HTO possess plate-like morphology with the surface smooth. And they display similar SAED patterns to HTO with [010]-crystal-axis vertical to the basal plane of them. It is surprised that Co-H₂O₂-HTO and Ni-H₂O₂-HTO show one set of diffraction rings with d -values of 0.281 and 0.243 nm except for one set of diffraction spots with similar d -values to H₂O₂-HTO. The diffraction rings of Co-H₂O₂-HTO and Ni-H₂O₂-HTO can be attributed to Co(OH)₂

and $\text{Ni}(\text{OH})_2$, respectively. On the contrary, the diffraction rings are not observed in $\text{Cu-H}_2\text{O}_2\text{-HTO}$, which may be due to without formation of $\text{Cu}(\text{OH})_2$.

Notes and references

1. Q. Feng, M. Hirasawa, K. Kajiyoshi and K. Yanagisawa, *Journal of the American Ceramic Society*, 2005, **88**, 1415-1420.
2. X. Kong, C. Zeng, X. Wang, J. Huang, C. Li, J. Fei, J. Li and Q. Feng, *Scientific reports*, 2016, **6**, 1-8.
3. H. Li, C. J. Firby and A. Y. Elezzabi, *Joule*, 2019, **3**, 2268-2278.